

Stability of high energy faults in Ni-based superalloys

Valery Borovikov¹, Mikhail Mendeleev², Timothy Smith³ and John Lawson²

¹*KBR, Inc., Intelligent Systems Division, NASA Ames Research Center, Moffett Field, CA, USA*

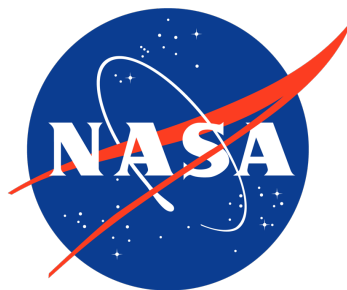
²*Intelligent Systems Division, NASA Ames Research Center, Moffett Field, CA, USA*

³*NASA Glenn Research Center, Cleveland, OH, USA*

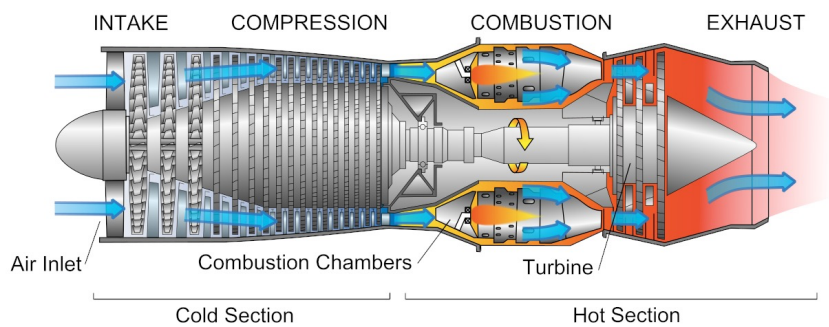
Support provided by

NASA's Aeronautics Research Mission Directorate (ARMD) –

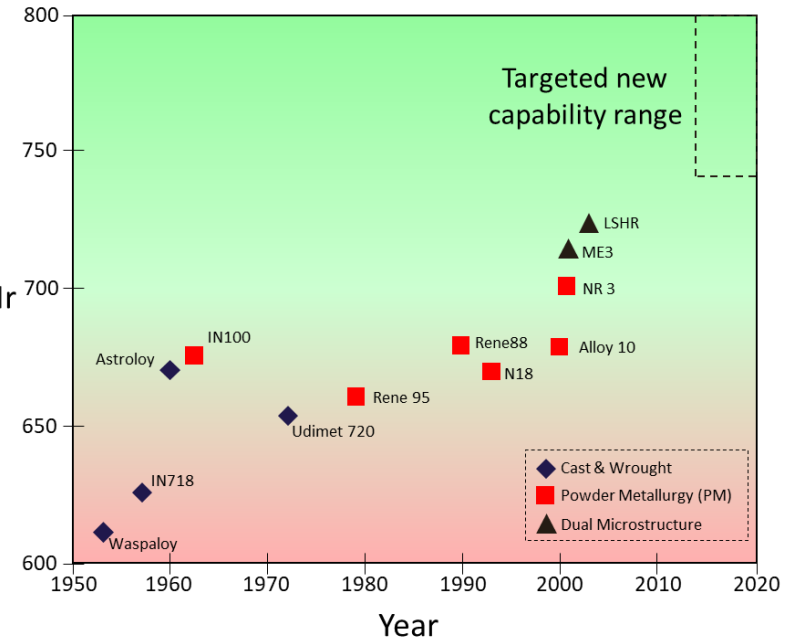
Transformational Tools and Technologies (TTT)



Progress in turbine disk alloys

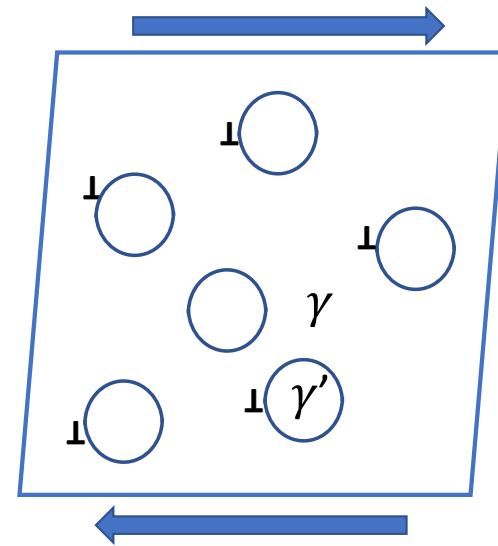
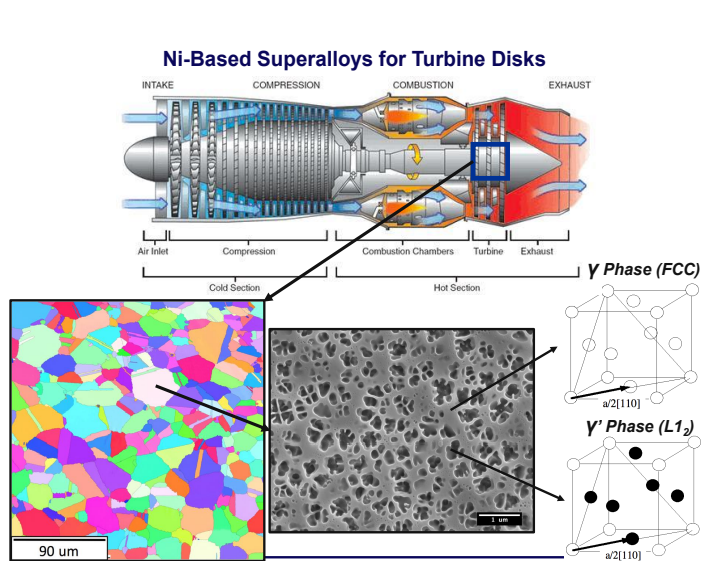


Temperature
Capability
690MPa/1000Hr
(°C)

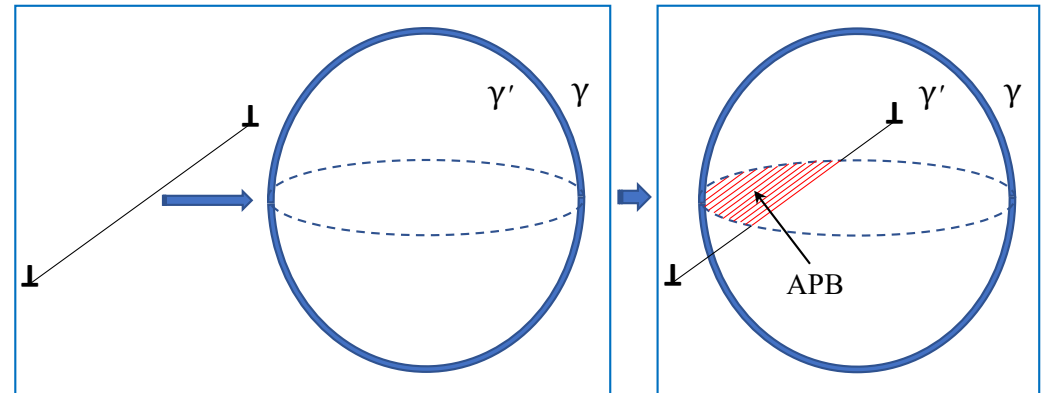
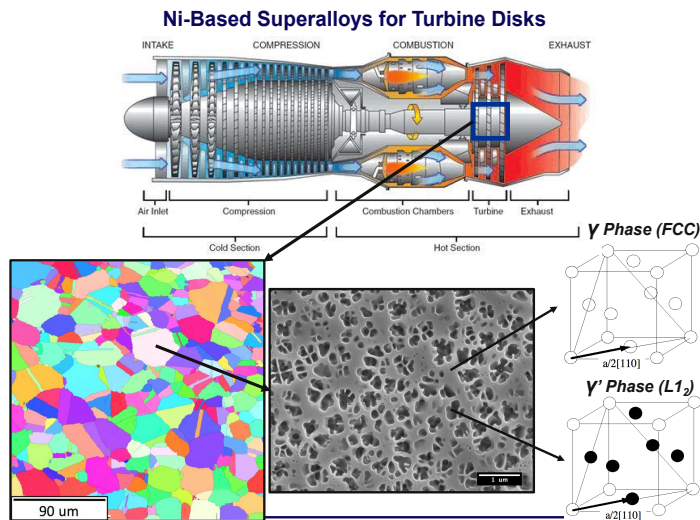


- Increase of the operating temperature of turbine engines is required to improve the efficiency and reduce the emissions.
- New deformation mechanisms (thermally activated) become important above 700 °C.
- Understanding the effects of microstructure and composition on functionality of these creep deformation mechanisms will lead to design of new materials with improved creep resistance.

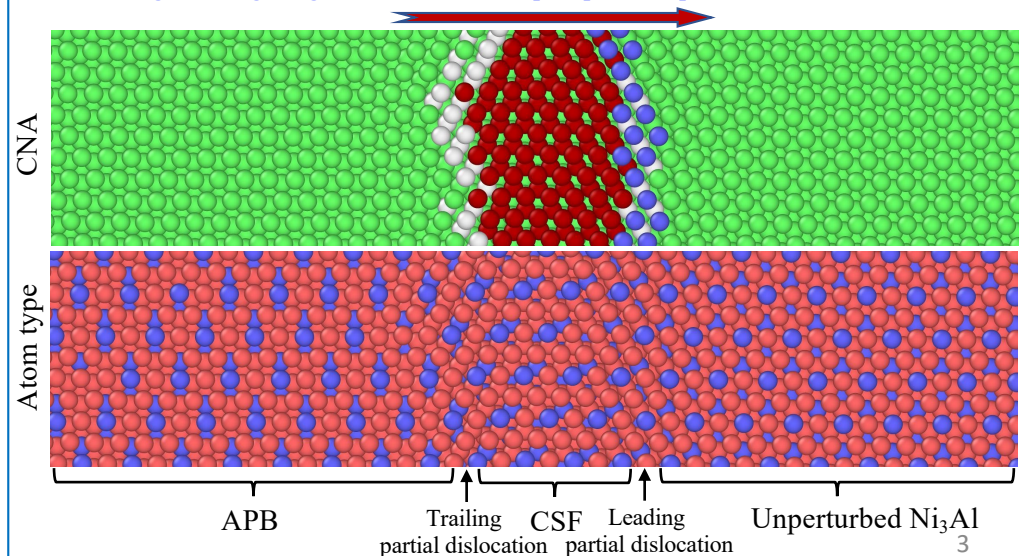
Deformation mechanisms in Ni-based superalloys



Deformation mechanisms in Ni-based superalloys

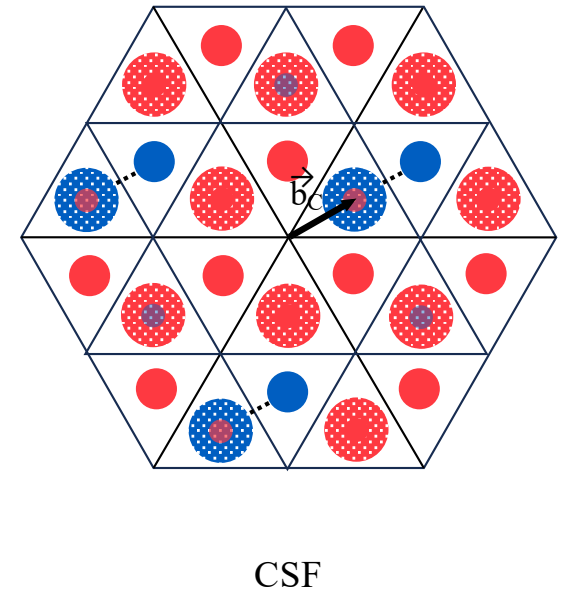
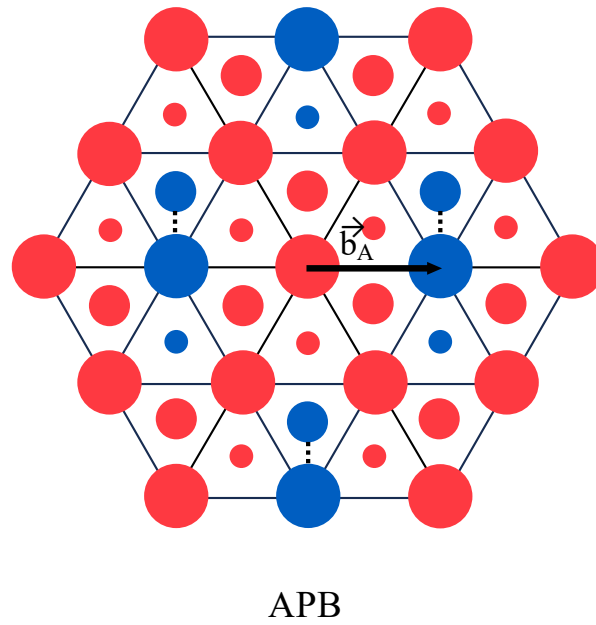
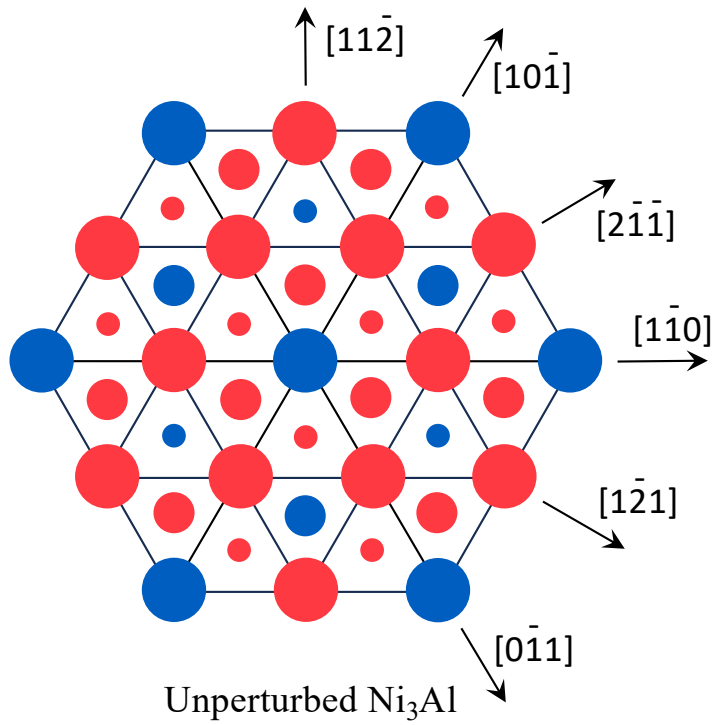


Passage of a single edge dislocation in Ni_3Al precipitate: unperturbed lattice \rightarrow CSF \rightarrow APB



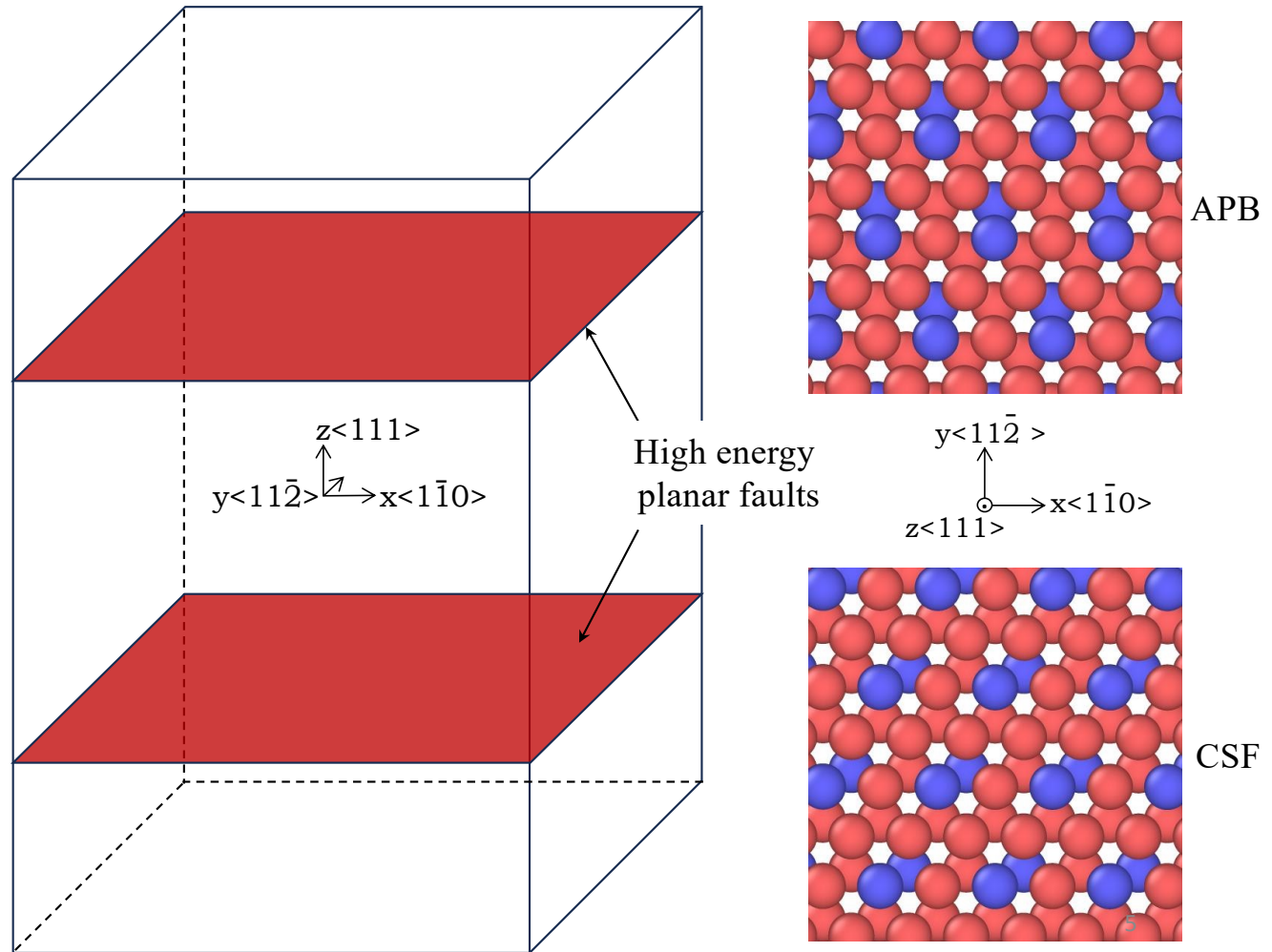
- Interaction of the dislocations with γ' precipitates is the main reason for high creep strength of Ni superalloys

Formation of high energy faults



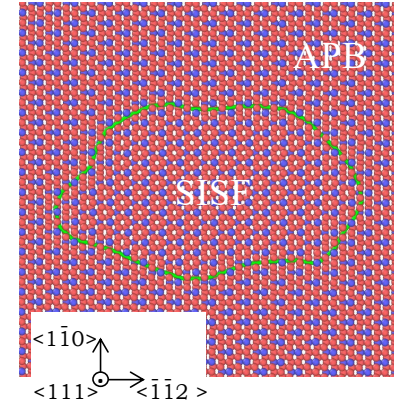
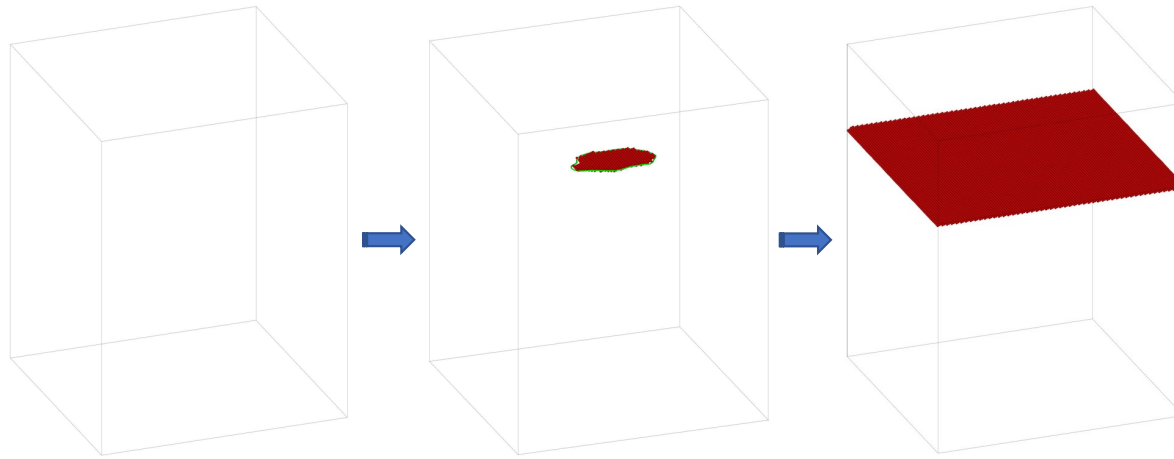
Simulation model

- $L1_2$ (Ni_3Al) with two high energy faults.
- LAMMPS package; Ni-Al-Nb interatomic potential by Mendeleev.
- Simulation cell size: $\sim 20 \times 20 \times 30 \text{ nm}^3$ ($\sim 1.1 \times 10^6$ atoms); PBCs in all directions.
- NPT ensemble (zero stress).
- Annealing at a target temperature for 0.3 ns.

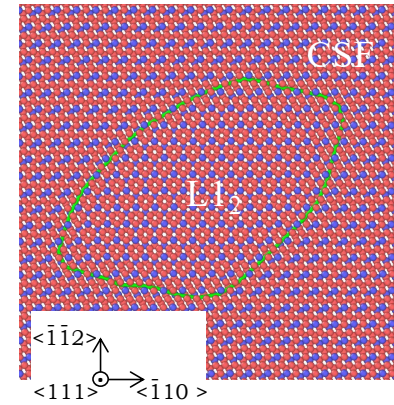
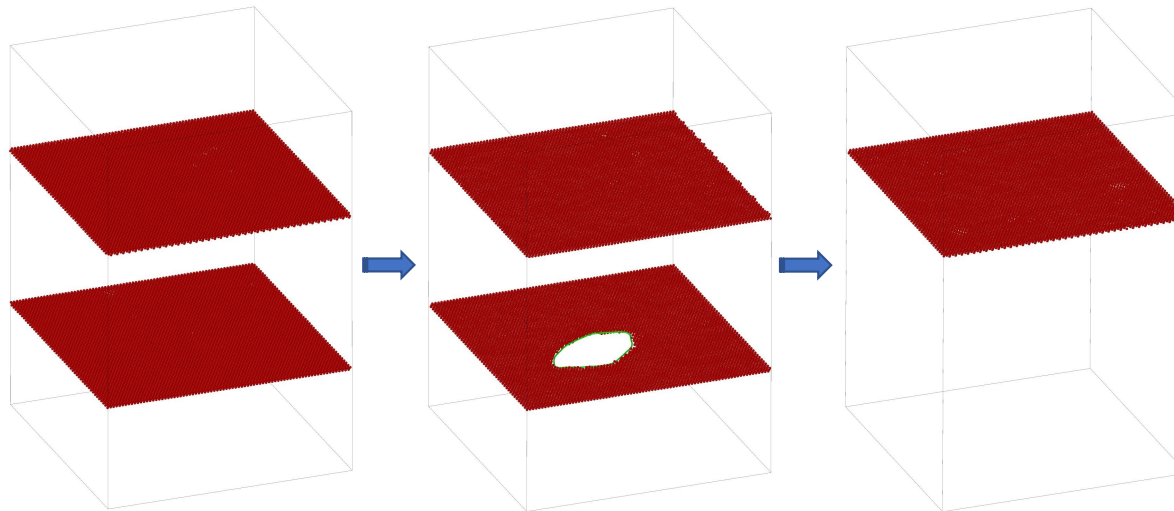


Spontaneous transformation of high energy faults

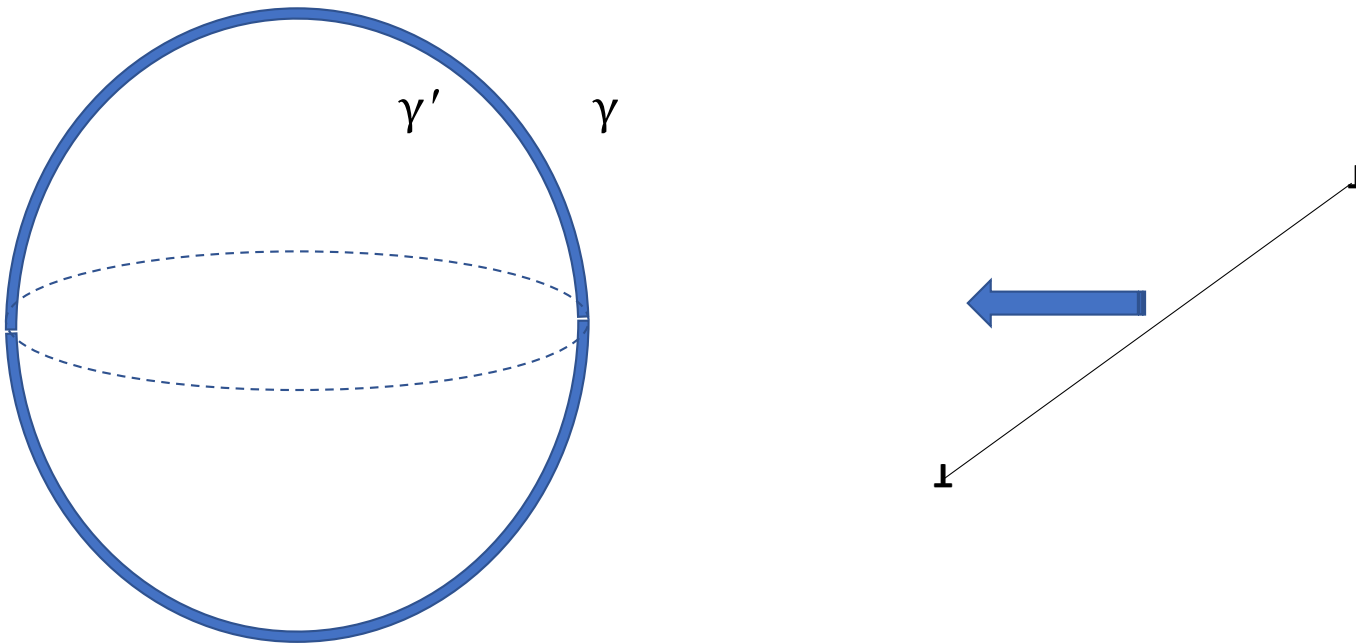
APB \rightarrow SISF
transformation
($T_{\text{APB} \rightarrow \text{SISF}} \sim 1120 \text{ K}$)



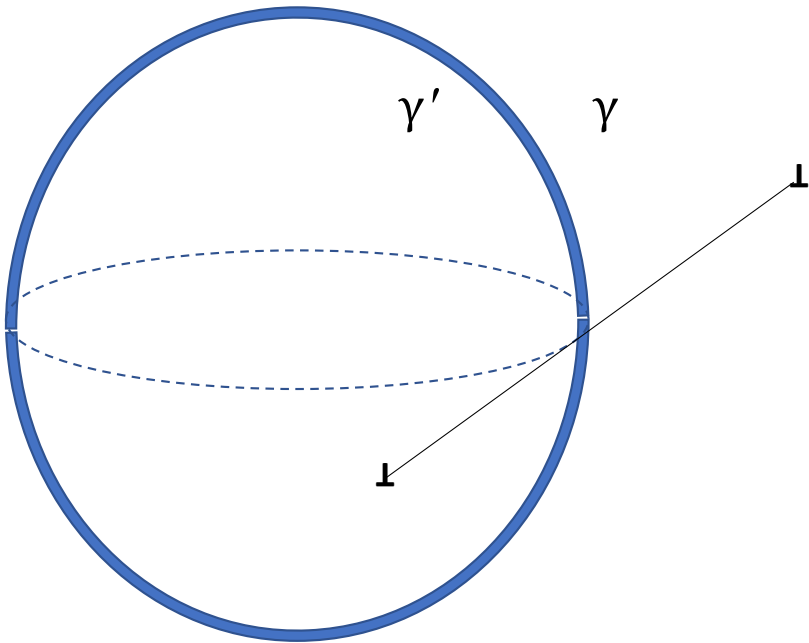
CSF \rightarrow $L1_2$
transformation
($T_{\text{CSF} \rightarrow L1_2} \sim 1057 \text{ K}$)



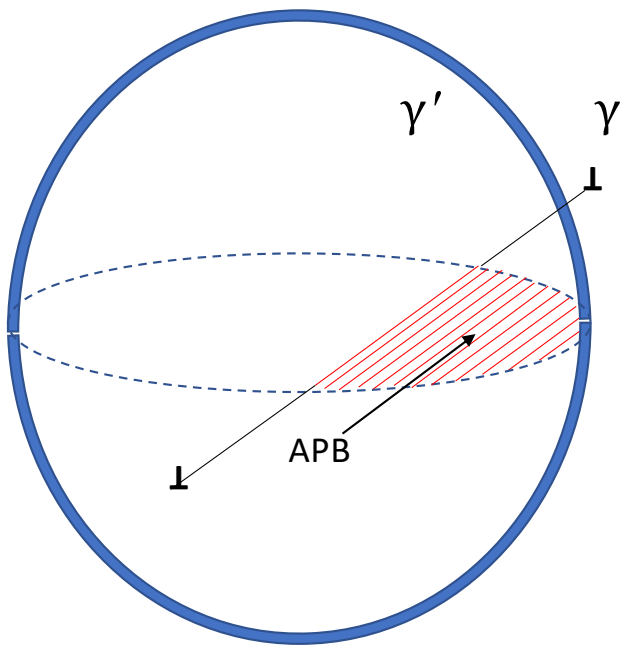
The Condat & Decamps mechanism of SISF formation



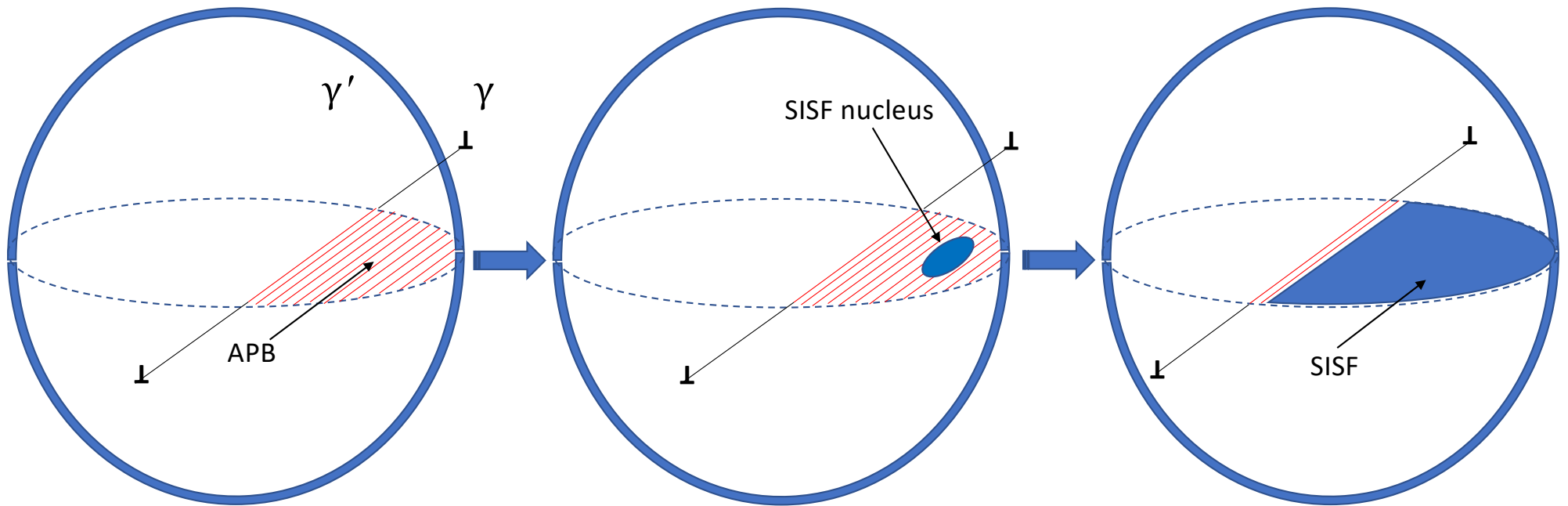
The Condat & Decamps mechanism of SISF formation



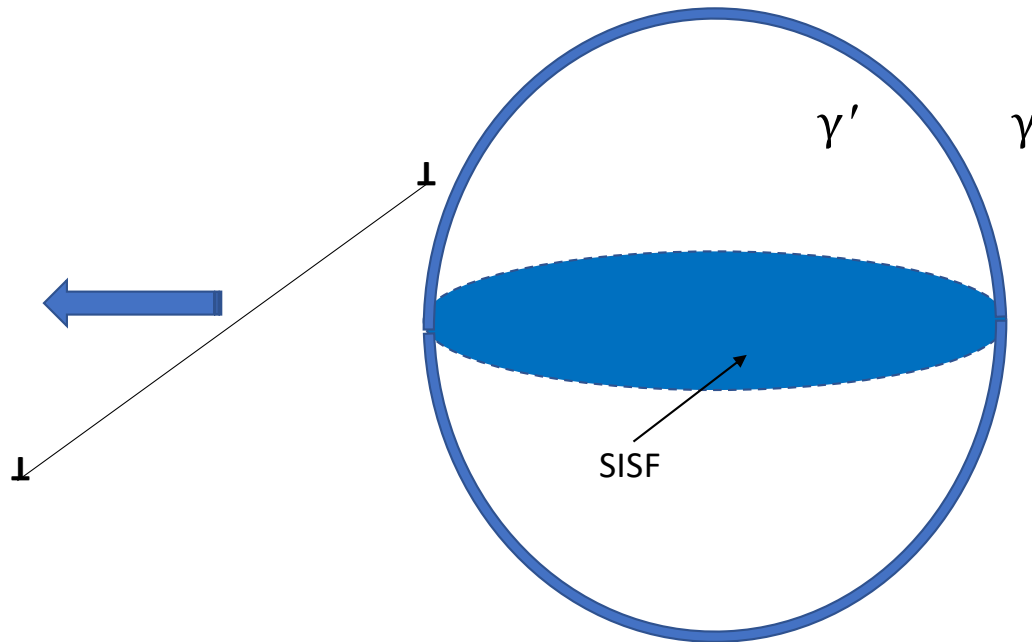
The Condat & Decamps mechanism of SISF formation



The Condat & Decamps mechanism of SISF formation

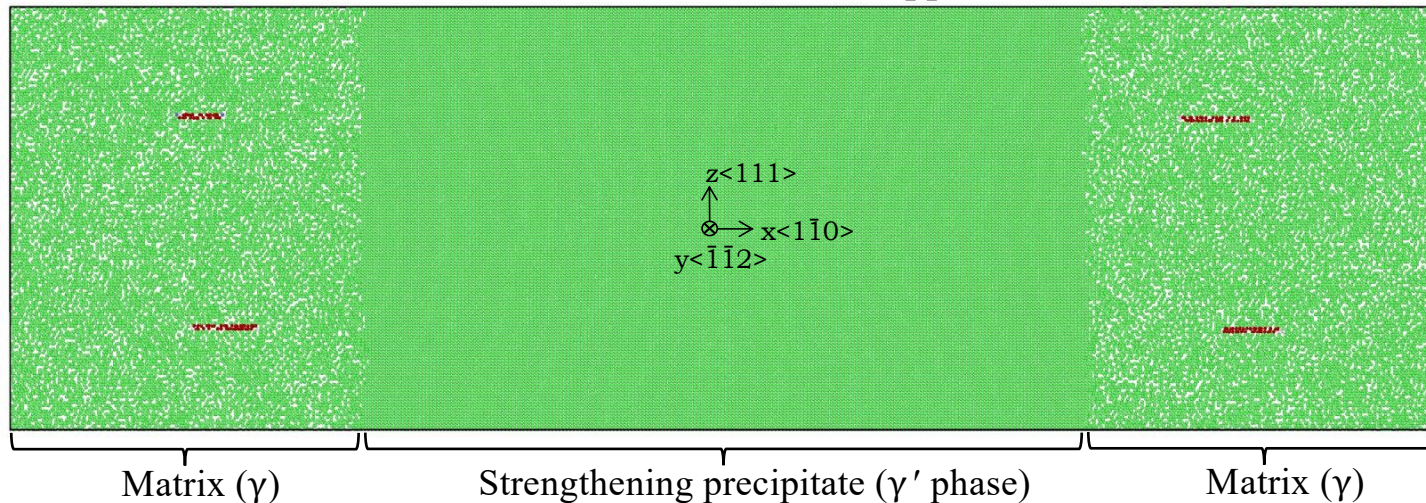


The Condat & Decamps mechanism of SISF formation

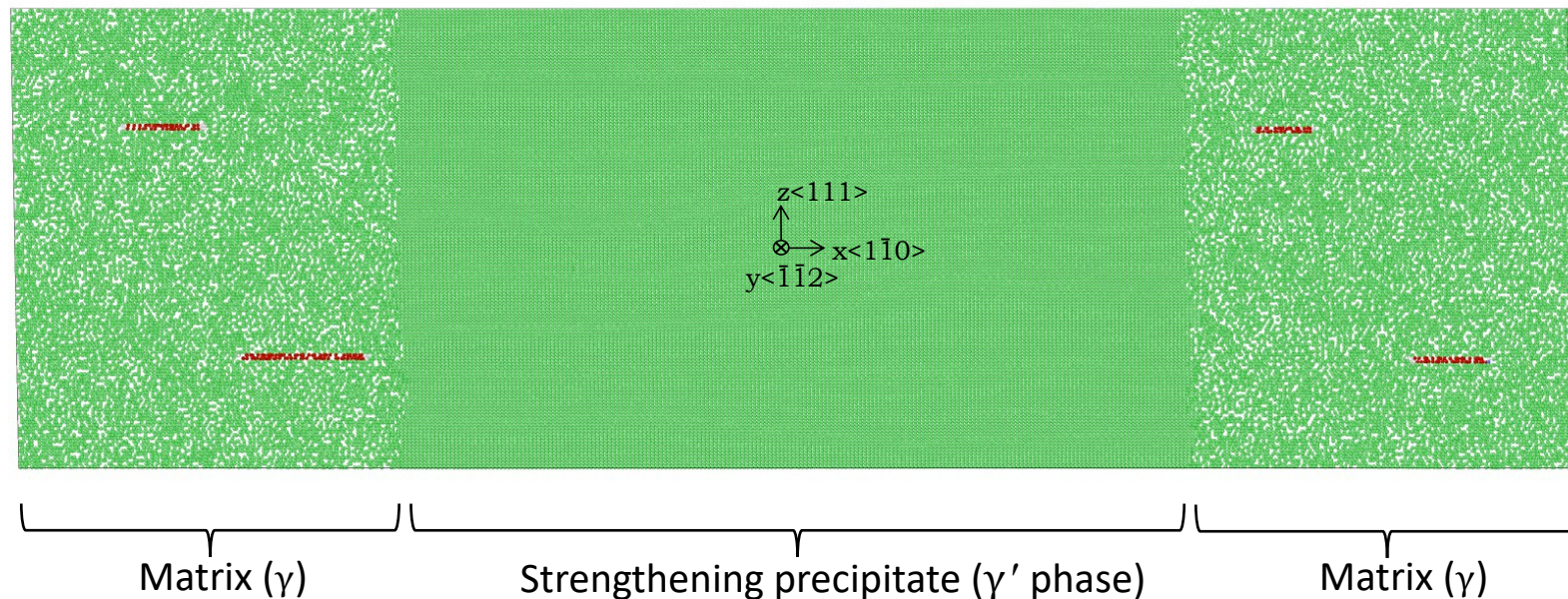


Simulation geometry and procedure

- Composite simulation system (Ni-Al), containing γ phase (matrix) and γ' phase (precipitate) regions and two edge dislocation dipoles.
- LAMMPS package; Ni-Al interatomic potential by Mendeleev.
- Simulation cell size: $\sim 100 \times 10 \times 30 \text{ nm}^3$ ($\sim 3 \times 10^6$ atoms).
- PBCs in all directions.
- The system was relaxed at $T = 1000\text{K}$, using hybrid MC/MD prior to introduction of dipoles.
- The dipoles were positioned in such a way that individual dislocations of upper and lower dislocation pairs would glide on adjacent $\{111\}$ planes when a σ_{xz} shear stress was applied.
- The MD deformation simulations were carried out under applied shear stress $\sigma_{xz} = 800 \text{ MPa}$.



Modified version of the Condat & Decamps mechanism of SISF formation



- The leading dislocation, entering the precipitate produces high energy APB inside the precipitate.
- Arrival of the second (trailing) dislocation to the interface triggers APB \rightarrow SISF transformation.
- APB \rightarrow SISF transformation significantly reduces the energy penalty associated with precipitate cutting.
- As a result, the deformation can progress further. The dislocation cuts through the whole precipitate, leaving an isolated SISF behind, and then escapes into the γ matrix.

Effects of solutes on the transformation temperatures

- The simulation system (Ni₃Al with two high energy faults), was modified by replacing 6% of atoms by Nb (Nb on Al-sites).
- Using the same procedure, we obtained the following transition temperatures: $T_{APB \rightarrow SISF}^{6\% Nb} \sim 1439$ K, $T_{CSF \rightarrow L1_2}^{6\% Nb} \sim 773$ K.
- Comparing with the results for pure Ni₃Al system ($T_{APB \rightarrow SISF} \sim 1120$ K, $T_{CSF \rightarrow L1_2} \sim 1057$ K), we can see that addition of Nb *increases* the temperature of spontaneous APB \rightarrow SISF transformation and *decreases* the temperature of spontaneous CSF \rightarrow L1₂ transformation.
- $\gamma_{APB} = 219$ mJ/m², $\gamma_{CSF} = 214$ mJ/m² and $\gamma_{SISF} = 62$ mJ/m².
- $\delta E_{APB} = \gamma_{SISF} - \gamma_{APB} = -157$ mJ/m² (APB \rightarrow SISF) and $\delta E_{CSF} = -\gamma_{CSF} = -214$ mJ/m² (CSF \rightarrow L1₂)

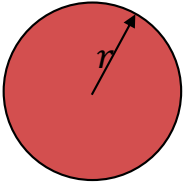
The change of energy associated with formation of a nucleus of radius r:

$\Delta E = \pi r^2 \delta E + 2\pi r \gamma_d$, where γ_d is the energy per unit length of the dislocation line surrounding the nucleus.

The energy of the critical nucleus: $\Delta E^* = -\frac{\pi \gamma_d^2}{\delta E}$. Assuming that γ_d is the same in both cases (APB and CSF), we can see that $\Delta E_{APB}^* > \Delta E_{CSF}^*$ and, therefore, $T_{APB \rightarrow SISF} > T_{CSF \rightarrow L1_2}$ in agreement with our MD simulation results.

$\delta E_{APB}^{6\% Nb} = -150.6$ mJ/m² and $\delta E_{CSF}^{6\% Nb} = -235.5$ mJ/m². Thus, $|\delta E_{APB}^{6\% Nb}| < |\delta E_{APB}|$ and $|\delta E_{CSF}^{6\% Nb}| > |\delta E_{CSF}|$.

Assuming that γ_d is not affected by the presence of Nb we obtain that $T_{APB \rightarrow SISF}^{6\% Nb} > T_{APB \rightarrow SISF}$ and $T_{CSF \rightarrow L1_2}^{6\% Nb} < T_{CSF \rightarrow L1_2}$ which is also in agreement with our MD simulation results.



Conclusions

- Using atomistic simulations, we demonstrate that the anti-phase boundary (APB) can spontaneously transform into super intrinsic stacking fault (SISF) and the complex stacking fault (CSF) can spontaneously transform into L12 lattice structure.
- The former transformation explains the experimentally observed presence of isolated SISFs and super extrinsic stacking faults (SESFs) in the precipitates.
- Multiple studies were focused on finding alloying additions which increase the APB and CSF energies.
- We demonstrate that alloying additions which increase stacking fault energies may conversely decrease their stabilities.
- This is important! If the high energy faults produced by lattice dislocations entering γ' precipitates can transform spontaneously into lower energy structures, then the strengthening effect due to second phase precipitates will be diminished.
- Further research into the effects of solutes on stability of superlattice faults in Ni-superalloys is required!